

Performance of UK Distribution Networks with single-phase PV systems under fault

Sivapriya BHAGAVATHY
University of Oxford – UK
sivapriya.mothilalbhadgavathy@eng.ox.ac.uk

Nicola PEARSALL
Northumbria University – UK
nicola.pearsall@northumbria.ac.uk

Ghanim PUTRUS
Northumbria University – UK
ghanim.putrus@northumbria.ac.uk

Sara WALKER
Newcastle University – UK
sara.walker@ncl.ac.uk

(Corresponding author: sivapriya.mothilalbhadgavathy@eng.ox.ac.uk)

Abstract— Faults are a major concern to the dynamic performance of distribution networks. With the predicted increase in PV contribution, it is vital to understand the impact of PV on the distribution network. However, there is very little work published that address the impact of PV systems on the dynamic performance of distribution networks. Most PV systems connected at the distribution level are single-phase in nature. A generic single-phase dynamic PV model, including the protection mechanism is presented in this paper. This enables the evaluation of the dynamic performance of distribution networks with multiple single-phase PV systems. The paper analyses the impact of faults on the PV inverter output using the models developed. The impact of PV on the network performance during fault is then analysed. The implications of the adoption of different regulations, viz. G-83, IEEE 1547:2018, IEC 61727 and VDE 0126-1-1, are also discussed. The results show that the presence of PV systems does not significantly affect the performance of the distribution network during faults. Also, the usual concern of loss of protection co-ordination does not occur at this voltage level. Faults that are far from the PV terminals would be cleared within 0.2 s. This indicates that the disconnection delay of 0.5 s as stipulated by G-83 is appropriate. However, a lower cut-off voltage for under-voltage disconnection than the current value stipulated in G-83 would enable more PV systems to stay connected during fault and avoid unnecessary loss of generation. The network used in this work is a representative of distribution networks and protection schemes in the UK. The results of this analysis are therefore extendable to any radial distribution network that use standard protection, e.g. fuses and relays in low voltage distribution networks.

Index Terms—distributed power generation, inverter-based generation, power system faults, power system protection, solar energy

1. INTRODUCTION

The fall in the price of photovoltaic (PV) systems over the last decade [1], together with government subsidies, has resulted in an increased number of PV systems being installed. Cumulative installed PV capacity in the UK reached 12.8 GW (end April 2018) across 947,980 installations [2]. The presence of PV may affect the steady-state and dynamic-state performance of the distribution network. Large currents and associated voltage sag in the distribution network during a fault can affect the system stability and cause further damage if action is not taken immediately to detect and disconnect a fault [3]. PV systems act as additional current sources that may contribute to the net fault current, thus affecting the distribution network performance as existing protection mechanisms may not be designed for this contribution. Research on the dynamic performance of power systems with a high

penetration of PV is relatively limited, with most work concentrating on the transmission level. These studies cannot be directly extended to distribution networks as the characteristics of a distribution system are very different from those of a transmission network (typically operating at voltages greater than 66 kV).

A number of studies have considered the impact of distributed generation (DG) on dynamic performance/fault performance [4-9]. However, they did not provide a clear differentiation between the types of generators and their different characteristics during a fault or a voltage sag. Experimental tests performed in Japan using a 200 kWp PV system and high resistance faults, to replicate faults at different distances from the PV, indicated that the substation overcurrent relay failed to detect the fault in many instances [10]. The ability of an inverter-based generation to disconnect within a few cycles after detection of a fault (fast disconnection) has been discussed in [5], with the requirement for extra care during the design of protection devices that rely on high fault currents. Further concern has been raised in [11] on the ability of the inverter to detect a fault and thus continuing to feed the fault, resulting in nuisance fuse operation. The report also observed that if the PV increases the fault current, the minimal melt time of the fuse may be reduced significantly, resulting in a lack of coordination with the upstream instantaneous trip mechanism. Malmedal et al. [12] discussed the impact of fault current contribution from the PV inverter on a 12.47 kV distribution feeder in the US and concluded that, at the residential level, the presence of PV has no impact on interrupting ratings of equipment. However, they assumed that inverters contribute to the fault current for less than 1 cycle under short-circuit, and feed around 1-2 times their rated current. Though they provided a detailed analytical approach to discuss the fault current contribution from rotating generators, the conclusion on PV inverters was drawn mostly from the assumptions on the characteristics of the inverter.

Results of testing a 1 kW single-phase 60 Hz inverter at the laboratory facility of NREL and at the manufacturer based on guidance given by the Underwriters Laboratories (UL) have been presented in [13]. Fault contributions from the inverter lasted between 1.1 – 4.25 ms (< 1 cycle) whereas the magnitude of fault current was 42.7 A, which is approximately 5 times the rated current. The test was performed only on one single-phase inverter and used a DC source of 16 kW rating which could have resulted in a higher current being supplied during a fault. Hence, this result cannot be directly extended to other single-phase PV systems. Le-Thi-Minh et al. [14] analysed two types of medium voltage distribution networks, rural and urban, prevalent in France with two PV systems rated 500 kW or 2 MW each and concluded that a fault in an adjacent feeder resulted in unnecessary tripping of PV in the healthy feeder. However, they do not discuss the reason for the drop of PV terminal voltages in the healthy feeder to near zero voltage for a fault in the adjacent feeder. Grumm et al. observed the fault current contribution of a three-phase PV inverter for faults with different resistances to earth representing fault at different locations of the network and concluded that the fault current contribution from PV systems can vary from 13 to 41% depending on the relative size of PV systems and the relative location of fault with respect to the location of PV systems [15]. However, the authors consider three-phase systems in distribution network which is atypical for the distribution networks in the UK. Katiraei et al. [16] used simulation-based and analytical methods to

calculate the contribution of PV inverters, rated 500 kW each, during faults and concluded that the contribution from PV is not a limiting factor. They categorised the inverters as fast disconnection type, which disconnected in less than 1 cycle under fault, and a generic model type, which took around 10 cycles to disconnect even when the voltage drops to less than 50% of the rated value. The fault current contribution from each inverter was assumed to be in the range of 1 to 1.2 times the rated current.

Traditionally, the fault current contribution from PV systems is ignored as this is comparatively smaller than the contribution from synchronous generators and also due to their fast disconnection on detection of fault [17]. The research on the impact of PV on distribution network during fault so far considers mainly medium voltage with the exception of [12], where loads are lumped on the 480 V distribution network. However, even this work does not discuss the protection present at 480 V, which is typically fuses, or consider details of the low voltage distribution feeder. Also, this work is for a network in the US, which operates under different standards of grid connection than those of the UK. The UK guidelines for connection of distributed generation (G-83) already gives longer time for tripping (around 25 cycles) than that stipulated by the IEEE guidelines of 0.16 s (usually considered in the literature).

This paper, therefore, aims to analyse the impact of multiple single-phase PV systems on an LV distribution network using an actual network in the UK and considers PV remaining connected for time durations as in G-83. The impact of fault at different locations of the distribution network on the PV system is also analysed. The impact of PV on the dynamic performance of the distribution network, which is becoming increasingly important given the growth in penetrations of PV in the distribution network, is evaluated in terms of the net fault current, net current at the distribution substation and voltage profile during a fault. The paper also discusses the implication of the different disconnection times (as stipulated by different guidelines) on the performance analysis which is highly relevant considering the recent discussions on fault ride through.

The contributions to knowledge made in this paper are:

- Development of a generic single-phase PV system model inclusive of the protection mechanism to replicate the dynamic behaviour of PV systems
- Evaluation of the dynamic performance of a three-phase residential feeder with multiple single-phase PV systems and domestic loads for single-phase to ground (SLG), double line (LL), double line to ground (LLG), three phase (LLL) and three phase to ground (LLLG) faults at different locations.
- Analysis of the implications of the adoption of different standards on the unwanted tripping of PV systems

The methodology used in this work, along with the different scenarios considered, is presented in section 2. This is followed by the details of the model developed for the analysis in section 3. Section 4 provides the results and discussion of the analysis together with the implications of the use of different regulations on the results of the analysis followed by conclusions in section 5.

2. METHODOLOGY

A representative of a typical distribution network in the UK, shown in Fig. 1, was chosen for the purpose of this study [18]. The network is in-line with the UK Generic Distribution System and is widely used by BEIS (previously DECC) to study the impact of distributed generation [19]. The network consists of a 33/11 kV substation with two 15 MVA transformers with on-load tap-changers supplying six 11 kV outgoing feeders. Each 11 kV feeder supplies eight 11/0.433 kV substations and each of them, in turn, supplies 384 houses through 4 feeders. As this research focuses on residential networks, one 11 kV feeder and one 0.433 kV feeder are modelled in detail as three phase line model using MATLAB/Simulink. The detailed 400 V feeder supplies 57 houses and it is assumed that these houses are uniformly distributed in the three phases across 6 node points (buses). The six nodes have 11, 8, 15, 4, 6 and 13 houses respectively. The details of the sample network are as given in Appendix A. The built-in dynamic load block in MATLAB/Simulink was modified to allow parallel operation of the load and PV. The after diversity maximum demand (ADMD) per house is 1.3 kVA at 0.95 pf lagging. From the department for business, energy & industrial strategy (BEIS)

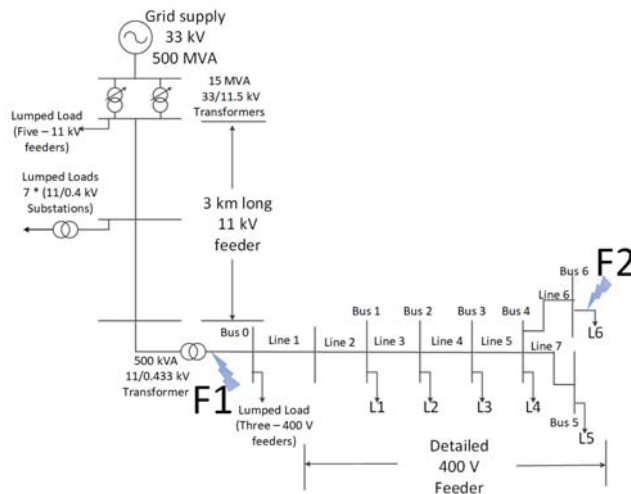


Fig. 1: Distribution network with fault locations F1 and F2 marked

statistics, the average rating of residential PV systems in the UK is around 2.9 kW [2]. The percentage penetration of PV is defined as the ratio of the total rated capacity of PV systems installed in the network to the ADMD of the network expressed as a percentage, as given in equation 1

$$\% \text{ penetration} = \frac{PV \text{ rating}}{ADMD * \text{no. of houses}} \quad (1)$$

For the purpose of this analysis, a self-clearing fault is introduced near the 11/0.433 kV substation and at the far end of the detailed feeder. The fault locations are marked in Fig. 1 as F1 and F2, respectively. The fault duration is considered as 1 s, as an intermediate value between the two trip times of 0.5 s and 2.5 s for different voltage drops stipulated by G-83/2 [20]. Simulations were performed for the following scenarios

- All fault types were covered: single-phase to ground (SLG), double line (LL), double line to ground (LLG), three phase

(LLL) and three phase to ground (LLLG)

- Two fault locations at F1 and F2
- PV penetration levels of 0% (representative of scenario with no PV), 40% (representative of scenario with maximum permissible penetration before reverse power flow occurs at 500 W load) and 100% penetration of PV system (representative of worst-case scenario with PV capacity equal to the ADMD of the network)
- PV distributed uniformly either near the substation or at the far end of the feeder
- Individual household load 500 W (value is not important for the current analysis, as the load has no significant impact on the performance during fault as shown by initial simulations as well as the literature [21])
- Solar irradiance of 400 W/m² (irradiance level is lower than or equal to this level for approx. 90% of sunshine hours in the UK [22]), 800 W/m² (irradiance level is higher than this for less than 5% of sunshine hours in the UK [22]) and 1000 W/m² (maximum irradiance usually considered in the literature).

The model of a PV system is as developed in section 3. Also, though the IEEE 1547:2018 allows the inverter to provide reactive power supply in case of voltages below 50%, it would take at least another 3-5 years before this is completely adopted by the testing bodies/manufacturers. This would imply that the distribution network will have a mix of PV systems disconnecting at different times and may/may not provide voltage support. Therefore, this study currently assumes that the single-phase inverters do not modify their reactive power output during a fault. It is usual when conducting dynamic analysis to consider system performance under worst-case scenarios, and if this is acceptable, then the system will be capable of handling the general operating conditions. From the results presented in section 4.2.1, it can be observed that the impact on fault current and substation current is higher for higher irradiance levels (close to 1000 W/m²) than lower irradiance levels. Therefore, the protection is evaluated for the standard maximum irradiance value of 1000 W/m². Also, the results of LLL and LLLG faults were similar as the transformer has earthed neutral.

3. MODELING AND SIMULATION

3.1 Model of a PV system in MATLAB Simulink

Surveys on commercial inverter topologies [23, 24], highlight that H-bridge is a common topology and that most of the low power commercial inverters do not use an isolation transformer. As the focus of the research is on developing a generic model of an inverter, rather than a model specific to a particular make or manufacturer, a common topology and control strategy is chosen. The model developed uses bipolar modulation as it produces reduced levels of low order harmonics [25]. The output voltage of a pulse width modulated (PWM) inverter is not purely sinusoidal and a filter is required to smoothen the waveform. The DC-link voltage should be greater than the peak AC voltage (325 V for 230 V RMS sine wave) plus the voltage drop across the inverter and the

AC filter. Hence the DC-link voltage is chosen as 425 V and the DC-DC boost stage provides a constant 425 V from the variable

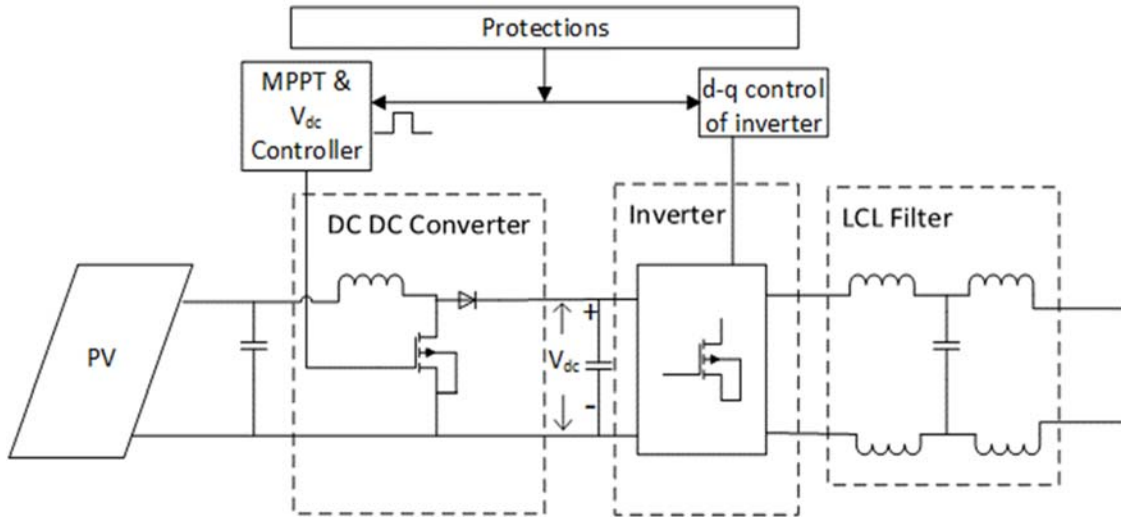


Fig. 2: Detailed block diagram of PV system

output voltage of the PV array. The detailed block diagram of the PV inverter is shown in Fig. 2. Phase locked loop (PLL) based method has been chosen for the generic model, due to the ease of use and availability of a built-in block in MATLAB Simulink. The load conditions usually change and the AC voltage output waveforms would have to be adjusted to the new conditions. Such adjustments can be made using a closed-loop approach which can use a feedforward or feedback approach. The feedback approach can compensate for the DC fluctuations and controls the gating signal depending on the deviation of the output of the inverter. The feedback control can be implemented via hysteresis current control or linear control. Hysteresis current control forces the AC line current to follow a given reference. The status of the switches is changed whenever the actual output current goes beyond a given reference. The drawbacks of hysteresis control for single-phase inverters are:

- a. Switching frequency cannot be predicted in a similar manner to the control using carrier-based modulators and therefore the harmonic content of the AC line voltages and currents become random. This is a disadvantage when designing the filter components.
- b. The controllers cannot fully eliminate the DC component in the load current in one waveform cycle.

Therefore, linear current control is used in the model developed. Linear controllers can be implemented using different reference frames viz. abc, $\alpha\beta$ (stationary) and d-q reference (rotating) frames. An error between the actual output current and the reference current is inherent in linear control while operating on abc or $\alpha\beta$ reference frame. The inherent error is due to the fact that the controller needs a sinusoidal error to generate sinusoidal modulating signals required by the modulator. This can be minimised by increasing the gain of the controller, which in turn increases the noise of the circuit resulting in the deterioration of the overall performance of the control scheme. To eliminate the steady-state error, rotating transformation based control is used, i.e. linear control in the d-q reference frame. The use of d-q frame also enables control of the real and reactive-power separately which would

allow the inverters to provide reactive power support if required. In a three-phase system, Clarke transformation is first used to transform the signal in the abc reference frame to the $\alpha\beta$ reference frame and Parks transformation is applied on the resultant signal to convert it into a d-q stationary reference frame. Parks transformation was first developed for three-phase signals and later extended to single-phase signals [26-29]. The $\alpha\beta$ components of a single-phase signal can be calculated using equation 4.2.

$$\begin{bmatrix} i_\alpha \\ i_\beta \end{bmatrix} = \begin{bmatrix} i_{\omega t + \varphi} \\ i_{\omega t + \varphi + \frac{\pi}{2}} \end{bmatrix} \quad (4.2)$$

where, i_α and i_β are the components of single-phase current along α and β axes of the stationary reference frame

$i_{\omega t + \varphi}$ is the single-phase output current of the inverter

$i_{\omega t + \varphi + \frac{\pi}{2}}$ is the phase-shifted single-phase output current of the inverter

That is, the original signal is complemented with an imaginary signal which is phase shifted by $\pi/2$ radians to create an orthogonal system similar to three-phase systems. These signals are then transformed to the d-q reference frame using

$$\begin{bmatrix} i_d \\ i_q \end{bmatrix} = \begin{bmatrix} \sin(\omega t) & -\cos(\omega t) \\ \cos(\omega t) & \sin(\omega t) \end{bmatrix} \begin{bmatrix} i_\alpha \\ i_\beta \end{bmatrix} \quad (4.3)$$

where, i_d and i_q are the d and q axis components of the current signal.

The output, ωt , of the PLL is used to perform the Parks transformation on the grid variable (i.e. grid voltage and current) to generate the respective d-q components. The d-q components of inverter current are passed through a low pass filter to eliminate the higher order harmonics introduced by the PWM controller in the signal. The direct axis current reference value is obtained from the DC-link voltage and DC reference value. The proportional-integral (PI) controller is reset on the rising edge of the external reset signal to mitigate the impact of controller saturation during a fault (detailed further in section 4.3). The output of the inverter is connected to an LCL (inductor-capacitor-inductor) filter before connecting to the grid to remove the harmonics in the voltage and current waveforms introduced by the PWM switching. The d-q controller of the inverter compensates for the voltage drop across the filter.

3.2 Over and under voltage protection

The PV inverter is designed to trip under different circumstances defined by the regulations/specifications pertaining to the respective country of use. As this research aims to evaluate the impact of PV on the dynamic performance of the distribution network, the under/over-voltage trip has been included in the generic model of the PV system developed. Fig. 3 shows the flow chart of the over/under voltage trip signal generation and the delayed resetting of the parameters. When the voltage at the terminals/point of grid connection goes beyond the normal range of values, the inverter trips within a delay depending on the magnitude of voltage sag/swell as stipulated by G-83[30] (Table 1). The signals are reset after a delay of 0.5 s which is smaller

than the delay in practical scenarios to ensure that the simulations are run faster. Fig. 4 shows the MATLAB/Simulink implementation of the over/under voltage protection.

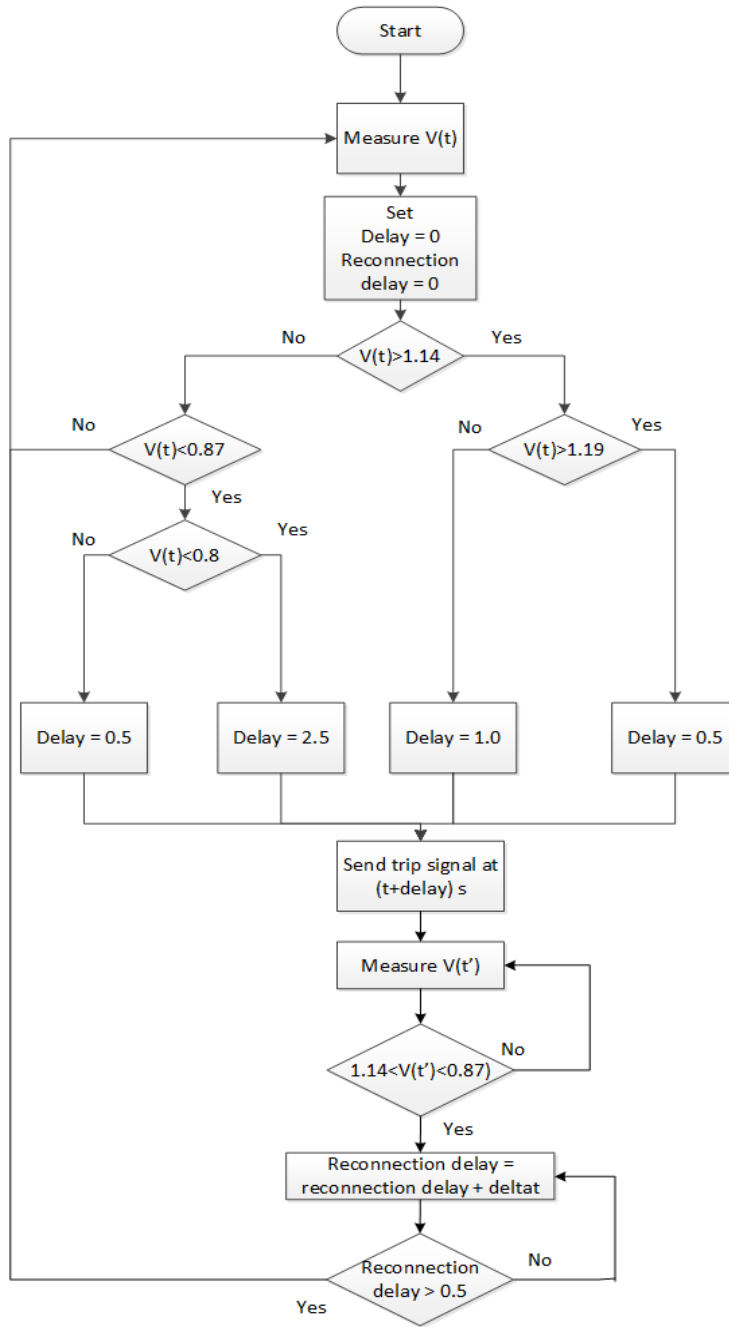


Fig. 3: Flow chart of Over/under voltage protection

3.3 Inverter control saturation during fault and modification thereof to the model

During a fault condition, the inverter disconnects from the grid due to any of the following factors: overcurrent at the AC side, excessive DC link voltage, loss of grid voltage synchronisation, reactive current injection imbalance [31], [32].

During fault or voltage sag, the operating point of the inverter deviates from the MPP as the power from the PV system is not fully transferred to the grid due to the voltage drop at its terminal. A problem that may appear because of the deviation of the operating point is that, after the fault is cleared, the DC-link voltage and the AC currents may take more than 3 s to reach the pre-fault values [32]. The reason is that the error in the DC-link voltage is accumulated in the ‘integral’ part of the PI controller. This accumulated value is limited by the current limiter and thus it has no effect on the grid currents. However, when the voltage sag ends, the excessive control action accumulated in the ‘integral’ part of the controller has to be compensated by an input error in the opposite direction. As a consequence, the DC-link voltage is reduced below the reference value. This may be overcome by using an anti-windup technique to stop the PI controller from accumulating the control action when it exceeds a specified value or using an external reset triggered by the fault clearance or voltage sag clearance. The model described in this section faced this issue when the simulations were carried out to understand the performance of the distribution network under fault. The output power of the inverter started to reduce almost 1s after the fault was cleared and went to almost zero before increasing again to reach the MPP power. An external reset was added to the current controller block, which resets the PI controller once the fault is cleared thus resolving the transients introduced by the accumulation of value in the PI controller.

3.4 Validation of the model

The two stages viz. the DC/DC controller with MPPT and the DC/AC inverter are validated individually as the published literature [33],[34] focussed on the performance of one of the two blocks at a time. As the generic model is not replicating any particular

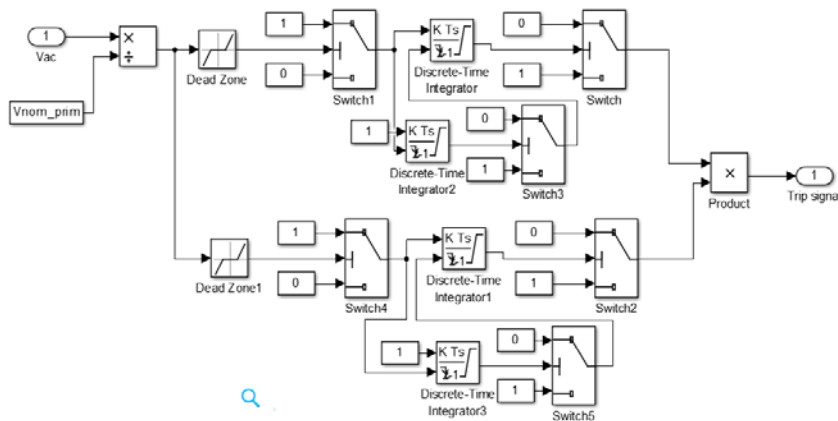


Fig. 4: Over/Under voltage protection of inverter

manufacturer, the fault current contribution from the PV inverter is modelled to be limited to 2 p. u., which can be changed if necessary by changing the upper limit of the PI controller in the d-q controller of the inverter. Also, the delay in tripping is set as equal to the maximum allowed time delay dependent on the voltage magnitude at the inverter terminals.

4. RESULTS AND DISCUSSION

A fault affects the performance of the PV system and the PV system may affect the performance of the distribution network during and after the fault. This section therefore first discusses the impact of fault on the PV output and then discusses the impact of PV on the different performance parameters of the distribution network. The results of scenarios with the highest impact on the performance parameter under consideration are presented in detail.

4.1 Impact of fault on the PV output current

The output current of the PV system is dependent on the voltage across its terminals and the irradiance level during the fault. Hence, the results are similar for the different types of faults considered. Fig. 5 shows the output current of a PV inverter in bus 1 for a fault at F1 for different irradiance levels of 400, 800 and 1000 W/m². The inverter takes around 10 cycles after reconnection to reach a steady state. The inverter output current has a first peak almost three times the rated current which is similar to the published experimental results in [35]. In [35], the inverter trips after the first peak itself. In the current study, in order to evaluate the impact of continued supply from the inverter for the maximum allowable duration mentioned in G-83, the inverter model was

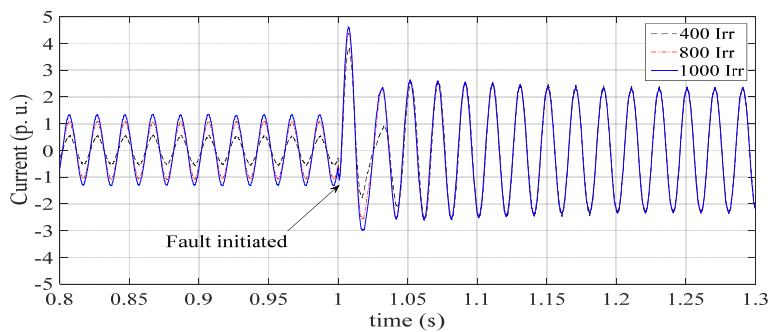


Fig. 5: Output current of an inverter at bus 1 for a fault at F1 for different irradiance levels

allowed to stay connected for a duration of 0.5 s after fault detection. It can also be observed from the figure that, though the magnitude of the first peak at 1000 W/m² irradiance levels is higher than those at 400 and 800 W/m², the continued contributions from the inverters are close to 2 p. u. (twice the rated current) irrespective of the irradiance levels. Most commercial inverters currently do not wait for the duration of 0.5 s before disconnecting from the grid in the case of a fault. However, if introducing LVRT, it is important to consider this continued contribution from the inverters for longer time durations.

Fig. 6(a) and (b) shows the output current of a PV inverter at bus 1 for a fault at F2 at 40% PV penetration and 100% respectively. At 40% penetration, the voltage at bus 1 is close to the boundary voltage of 0.8 p.u. (0.804 p.u.) and hence the inverter trips after 0.5 s of fault occurrence. However, for the similar conditions at 100%, the voltage at bus 1 is 0.82 p.u., higher than the limit of 0.8 p.u., and therefore the inverter stays connected for the 1 s duration as shown in Fig. 6(b). Table 1 gives the cut-off voltages and the delay times.

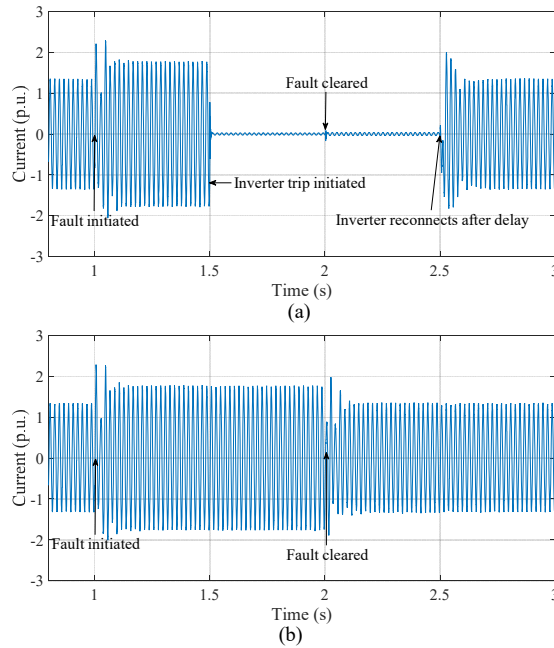


Fig. 6: Instantaneous output currents of PV inverter at bus 1 for a fault at F2 for different penetration levels of PV: (a) 40% and (b) 100%

Fig. 7 shows the output current of the inverter from 0.1 s before and after the fault. It can be observed that the peak, as well as the continued contribution of fault current from the PV, increases with an increase in irradiance. The decrease in contribution is more pronounced for a fault at F2 than for a fault at F1. For a fault at F1, the lumped PV also trips within 0.5 s as the voltage across one of the phases is lower than the limits in G-83. This is unlikely in practice, where the PV would be single phase in nature and distributed across the three phases, resulting in disconnection of inverters connected to phase A but not others connected to other phases. For a fault at F2, the lumped PV experiences only a voltage sag and remains connected to the network. This is similar to a practical scenario, where fault at F2 is representative of a fault in the adjacent feeder, for which the inverters should not trip, or trip only on a sustained voltage sag. The disconnection of PV systems due to faults result in a generation loss for a minimum of 300 s (minimum disconnection delay). Hence it is preferred that PV systems do not trip unnecessarily.

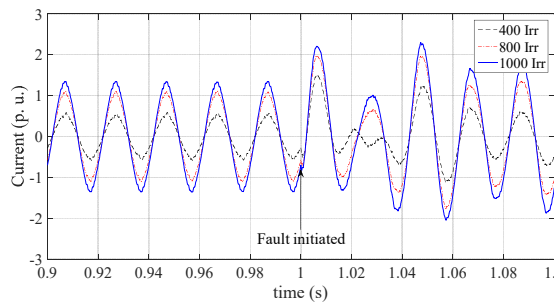


Fig. 7: Output current of PV inverter in bus 1 for a fault at F2 for different irradiance levels

4.2 Impact of PV on the distribution network

The presence of PV may affect the settling time, net fault current, net current at the substation, voltage profile during a fault, and the protection mechanism. The impact of PV on the settling after a fault due to reconnection of the PV systems is shown to be insignificant and is not discussed further.

4.2.1. On net fault current

For a fault at F1, the presence of PV systems increases the net fault current at the point of fault. However, the increase is minor and can be considered as negligible for both 40% and 100% penetration of PV systems irrespective of the location of PV systems for the different types of faults considered. Also, the level of irradiance has no significant impact on the net fault current for a fault at F1. For a fault at F2, the increase in net fault current is dependent on the location of the PV systems and on the type of fault as shown in Fig. 8(a) and (b). When the PV systems are considered to be distributed at the far end of the feeder, the net fault current for SLG fault increases by 6% and 13% for 40% and 100% PV penetration respectively. However, if the PV systems are considered to be distributed closer to the substation, then the increase in net fault current for SLG fault is around 1% and 6% for 40% and 100% PV penetration. The net fault current is also dependent on the irradiance level during the fault. The net fault current increases with an increase in irradiance at the given penetration level for a fault at F2 as shown in Fig. 8(a). The net fault current is highest for SLG fault and lowest for LL fault.

4.2.2. On net current at the secondary of the substation

The presence of PV does not significantly affect the net current at the substation during the fault for a fault at F1. The presence of PV decreases the net current at the substation from 25 kA to 24.6 kA i.e. about 2% decrease for a SLG fault. For a SLG fault at F2, the net current at the substation for 0, 40 and 100% penetration of PV systems with PV systems distributed near the substation is as shown in Fig. 9(a). At 40% penetration, the current at steady-state is close to zero as most of the load is met by

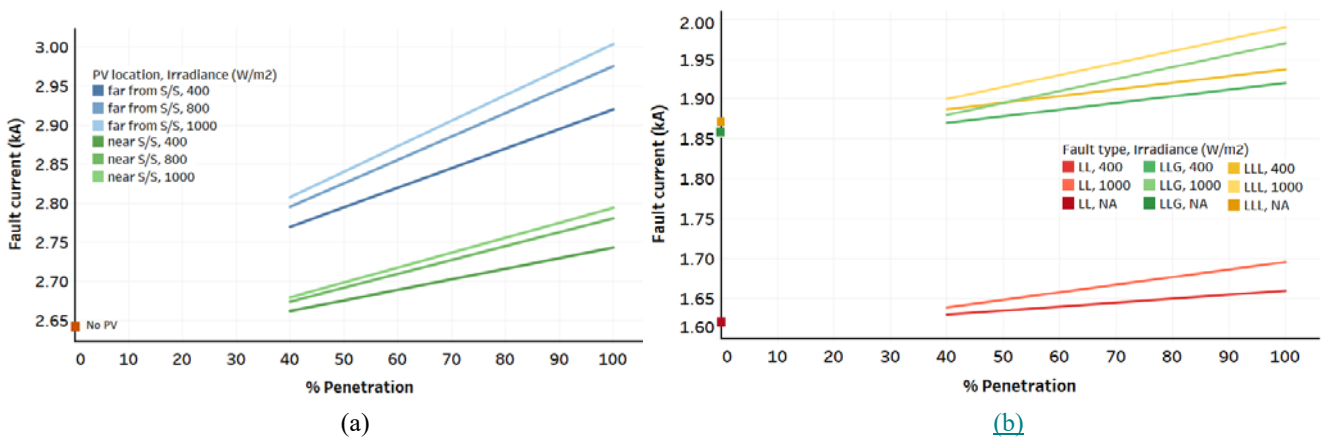


Fig. 8: Net fault current for different types of faults, penetration levels and different irradiance levels for a fault at F2 - (a): Single line to ground fault; (b): Double line fault, double line to ground fault and three phase fault

the PV. The fault is initiated at 1 s and, after 0.5 s delay, the inverters connected to bus 1 disconnect from the network as the voltage at bus 1 is around 184 V (the boundary voltage as per G-83). This results in a slight increase in the current drawn from the substation, as shown in Fig. 9, as the fault current that was being supplied by the inverter, is now supplied by the substation. However, the lumped PV remains connected to the grid as it experiences only a voltage sag. Therefore, the net current at the substation during fault at 40% penetration of PV is not the same as the no PV scenario for the duration from 1.5 s to 2 s. The fault is cleared at 2 s, the inverters at bus 1 reconnect to the network after a delay of 0.5 s and the network returns to the steady-state conditions with a minor impact on current. The current during steady-state at 100% PV penetration is higher than the current with no PV, as at this penetration level current is being fed to the substation (generation higher than load). Similar to the 40% penetration level, the inverters connected to buses 2 and 3 disconnect after a delay of 0.5 s resulting in an increase in current supplied by the substation after 1.5 s. However, the PV systems connected to bus 1 remain connected to the grid as the voltage is higher than 184 V and the lumped PV systems also remain connected to the distribution network. During the fault, the net current at the substation decreases from 3000 A (peak) at no PV to 2600 A (peak) and 2100 A (peak) at 40% and 100% PV penetration respectively i.e. a reduction of 13% and 30%. The reduction in current at the substation remains at similar percentages for PV distribution at the far end of the feeder for a fault at F2. The net current at the substation during fault at a given PV penetration is also dependent on the irradiance level during a fault. At a low irradiance level of 400 W/m², the decrease in substation current is only around 5% as against 13% at a high irradiance level of 1000 W/m², for 40% PV penetration. A similar trend is also visible for a LL fault as shown in figure 9(b). However, for a LL fault, not all inverters trip after 0.5 s for both 40 and 100% PV penetration.

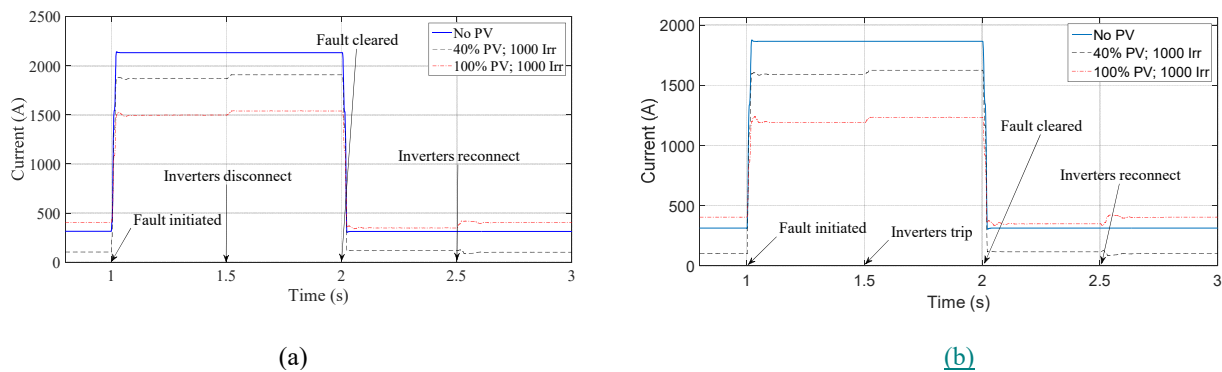


Fig. 9: RMS current at the secondary of the substation for 0, 40 & 100% PV penetration of PV systems near the substation for a fault at F2 – (a) SLG fault; (b): LL fault

4.2.3. On voltage profile during fault

Since SLG fault introduces highest unbalance, this section focusses on the results of this fault. When a SLG fault occurs at F2, the voltage in phase A at the substation drops from a steady state voltage of 247 V (1.07 p. u.) to 232 V (1.01 p. u.), 232.7 V (1.01 p. u.) and 235.5 V (1.02 p. u.) for 0%, 40% and 100% PV penetration, respectively as shown in Fig. 10. For a similar

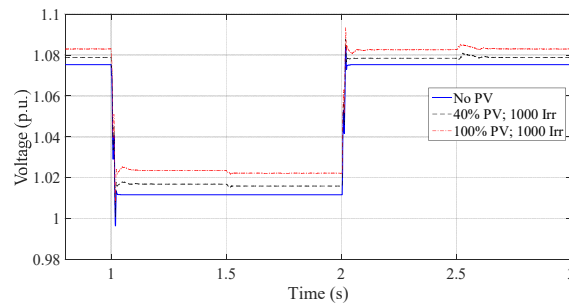


Fig. 10: RMS voltage in phase A at substation for a fault at F2 for different penetration levels of PV with PV distributed near the substation and irradiance of 1000 W/m^2

fault but with PV distributed at the far end of the feeder, the voltage in phase A at the substation for 40% PV penetration is 1.016 p. u. (233.8 V) i.e. 0.5% higher than when the PV was distributed close to the substation. For a fault at F1, the voltage drops to near 0 during fault irrespective of percentage penetration and distribution of PV systems. For an SLG fault in phase A, the voltages in phase A across the distribution network are not significantly affected by the presence of PV systems. However, at 100% penetration, there is a slight over-voltage in phases B and C at buses 4, 5 and 6, as shown in Fig. 11 (voltage in excess of 1.1 p. u.). This may be due to the presence of the three-phase lumped PV system where the voltage sag on one phase affects the voltages across the other two phases and the resultant currents. Overvoltage in healthy phases during a SLG fault has been raised as a concern in [12]. At 100% penetration of PV, the voltage at bus 1 during a fault is higher than 184 V which means that the PV systems remain connected to the network for 2.5 s. However, if the PV systems were following the German regulation VDE 0126-1-1, those connected to bus 1 would be disconnected for 40% and 100% penetration levels for a fault at F2. If the PV systems were following the European regulation IEC 61727 or the US regulation, the voltage level at which the PV systems should disconnect is 50% of the rated voltage. This indicates that PV systems at bus 1 and bus 2 would remain connected to the grid for both the penetration levels irrespective of the location of the PV system with respect to the substation for a fault at F2. The voltage profile of phase A, during a fault at F2 for different penetration levels of PV systems distributed near the substation, is as shown in Fig. 12. The dotted lines at 0.8 p. u. and 0.5 p. u. indicate the boundary conditions

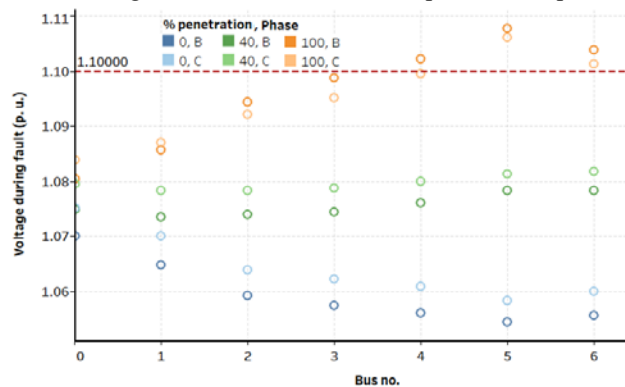


Fig. 11: Voltage in the healthy two phases during a fault on phase A at F2 for 100% penetration

for disconnection of the PV system in the event of under voltage as given by G-83 and IEC/US regulation. While evaluating the impact of PV on the distribution network performance, it is important to consider the regulations adopted.

4.2.4. On network protection

The impact of PV on the fault clearance times and co-ordination between relays, resulting in an incorrect operation, has been raised as a concern in the literature. Fault clearance times typically range from <0.1 s to 1 s or more depending on the fault level and the protective device used. At the distribution level, in particular at less than 11 kV, the protection mechanism is largely dependent on fuses and simple over-current relays. The technical recommendations at this voltage level is typically around the increased capability of inverters to handle faults (low voltage ride through) rather than the replacement of fuses/relays due to the economics and time of disruption to customers during such a replacement. Hence, advanced adaptive protection schemes are not considered. Relays at different voltage levels and in different sections of a distribution network use time grading to distinguish the faults in different sections of the network. For time grading, the operating time for the protective equipment at the lowest voltage level is chosen first and a margin of 0.4 s or 0.5 s is added to each stage back to the main station/grid [36]. For the network under consideration, the lowest voltage level is 400 V with protective equipment of fuses and at 11 kV there are four relays in sequence resulting in a delay of 1.8 to 2.2 s at the grid supply relay. Theoretical calculations for fault currents arising from a fault at F2, under no PV scenario, yields a minimum fault current of 1.9 kA with one supply transformer disconnected (typical process to calculate minimum fault current for the design of relays).

To achieve discrimination between fuses in series, the network operators typically use the same type of fuses with a ratio of ratings of the two fuses not less than 2. For the distribution network under consideration, the service feeders usually use 35 mm^2

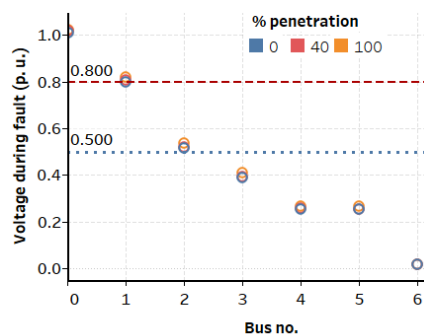


Fig. 12: Voltage profile of A phase, during fault at F2 for different penetration levels of PV systems

combined neutral earth conductor (CNE) and the service feeder for each house is provided with a fuse of 60 A rating for a single-phase residence. Heavy duty fuses rated at 200 A are typically used in each branch of the 400 V distribution network [37]. Energy Networks Association Technical Specifications (ENATS) 37 -2 recommends that the fuse used in single transformers up to 500 kVA rating should be capable of withstanding 18 kA fault current for up to 0.5 s [38]. The code of practice of Northern Power Grid (UK) [39] provides a guidance on the selection of fuses at a substation that, for a 500 kVA

substation, a 500 A fuse is used at the low voltage side and 40 A expulsion fuse is used at the high voltage side. However, Electricity Northwest limited (UK) uses a 400 A and 25 A fuse respectively at low and high voltage sides of the transformers [40]. The difference could be attributed to the ratings of the cables used or the load served by the respective network operators. The time-current zones of low voltage fuses of different ratings are given in [41].

For a fault at F2, which represents a fault at any individual house/load, the 60 A fuse at the service head trips within 0.1s irrespective of the contribution of PV. If the fault at F2 represents a location on the branch between bus 4 and bus 6, the first protection mechanism to work would be the 200 A fuse near bus 4. Fault current of 1.6 kA (at no PV, LL fault) would trip the fuse the 200 A fuse within 0.3 s. With PV, even a 1-2% increase in net fault current would result in faster tripping of this fuse. The fuse at the low voltage side of the transformer can also be considered as a backup protection for a fault at the far end of the feeder. For a 400 A fuse, the operating time changes from 4 s under a no PV scenario to 8 s and 20 s under 40% and 100% PV respectively for a LL fault. If a 500 A fuse was used with the transformer this change is reflected in a change in operating time from 11 s under a no PV scenario to 20 s and more than a minute under 40% and 100% PV respectively for a LL fault. Though the probability of failure of all the fuses in each branch is very low, the change in operating time for a 500 A fuse is significant as a typical time-delay of operation of the fuse in a low voltage network varies from 30 s to 60 s [42]. For a fault at the secondary of the substation, the secondary substation will trip within 0.1 s irrespective of the PV penetration or type of fault.

4.3 Implications of different regulations on the unwanted-tripping of PV systems

Table 1 shows the voltage ranges at which the inverters should disconnect and the respective disconnection times as per the different standards. Typical relay disconnection time is around 0.2 s maximum and the following reclosing occurs after a typical delay of 15 s to check whether the fault is permanent or not. For a fault at F1, the relay would disconnect the feeder within 0.2 s resulting in a voltage drop to zero and, before the next reclosing, the inverters would have disconnected. Therefore, a time delay of 0.5 s for a fault at F1 is sufficient. For a fault at F2, the relay is the backup protection, which would act with a delay of 3 s or 6 s depending on the transformer protection under no PV scenario. If the voltage sag lasts more than 0.5 s, it indicates that the local protection mechanism close to the fault failed to operate, requiring the backup protection to act, within 0.7 s (adding the time grading between fuses). So the inverter that disconnects within 2.5 s allows ample time for the backup protection to act. However, if that fuse also fails to act and the fuse at the secondary of the substation has to act. Disconnecting within 2.5 s would still allow the relay to pick up the fault. This implies that the time delays considered in G-83 are sufficient for the protection mechanism in distribution networks in the UK.

Table 1: Comparison of disconnection times as per different standards of PV connection to the grid

Standard	Parameter	Voltage range (%)	Disconnection time (s)
G-83 [30]		$80 \leq V_{ph-n} < 87$	2.5
		$V_{ph-n} < 80$	0.5
		$114 \leq V_{ph-n} < 119$	1.0
		$V_{ph-n} > 119$	0.5
IEC 61727 (Europe) [43]		$V < 50$	0.1
		$50 \leq V < 85$	2
		$110 < v < 135$	2
		$V \geq 135$	0.05
IEEE 1547:2003 (USA) [44]		$V < 50$	0.16
		$50 \leq V < 88$	2
		$110 < v < 120$	1
		$V \geq 120$	0.16
IEEE 1547:2018 (USA) [45]		$V < 50$ (may be required to provide reactive power support)	<0.16
		$50 \leq V < 70$	0.16
		$70 \leq V < 88$	$0.7 + 4 \times (V \text{ p.u.} - 0.7)$
		$115 < V \leq 117.5$	0.5
		$117.5 < V \leq 120$	0.2
		$V > 120$	0.16
VDE 0126-1-1 (Germany)		$50 \leq V < 88$	2
		$110 < V < 120$	1
		$V \geq 120$	0.16

Fig. 12 shows the voltage profile for a fault at F2 and it can be observed that the lower boundary condition of 50% voltage sag would enable more PV systems to stay connected in the event of a fault at F2. The boundary condition of 50% voltage drop stipulated by IEC would enable the PV systems to be connected for longer duration (2 s) for a fault further away from the PV system, which could be representative of fault at the far end of the feeder when PV is located close to the substation or a fault at the adjacent feeder. Disconnection of the inverter for a voltage sag due to a fault in an adjacent feeder is undesirable as it leads to generation loss and may result in a further drop in voltage. Though the IEEE standards (2003 and 2018) provide lower cut-off voltages of 50% than G-83, the time for disconnection may not be sufficient for the backup protection in distribution networks to act, resulting in disconnection of a higher number of PV systems which in-turn increases the voltage drop.

5. CONCLUSIONS

The fault current contribution of PV inverters has generally been ignored, owing to their fast disconnection times and relatively lower currents than for the synchronous generators. However, with an increasing contribution from PV at residential levels and longer disconnection times, it is important to understand the impact on protection systems at low voltage levels. Also, as the UK guidelines for inverters provide a longer disconnection delay than the IEEE standards, it is important to understand the performance

of inverters that take longer to disconnect. This is also particularly relevant given recent discussions of LVRT. This paper presented a generic model of a PV system including the protection mechanism. The paper then presented the impact of fault at different locations of the distribution network on the PV systems and the impact of PV systems on the performance of the distribution network during and after a fault. The performance of the distribution network during a fault is evaluated in terms of the net fault currents, net current at the secondary of the substation transformer and the voltage profile during a fault. The impact of the lumped PV system representing PV in adjacent feeders is also presented. The impact of PV systems on the protection mechanism in the distribution network is considered. The impact of the use of a different guideline from G-83, specifically the IEC/US guideline, to determine the disconnection of the PV system during a fault is also presented.

For a fault close to the substation, irradiance level has no significant impact on the net fault current or fault current as seen by the substation. The fault current as seen by the substation decreases with increasing penetration of solar PV for all types of fault at the far end of the feeder. The impact is higher for irradiance levels closer to 1000 W/m^2 than at lower irradiance levels. The reduction of current at the substation during fault at the far end of the feeder may significantly increase the tripping time of the fuse at the 11/0.4 kV substation and also result in lack of coordination with the relay at the primary. However, for a fault at F2, fuses at all the branches from the location of the feeder to the substation will provide backup and it is very unlikely that the fuse at the substation would trip. That is, irrespective of the irradiance levels, the occurrence of this event is highly unlikely.

The network used in this work is a representative of distribution networks and protection schemes in the UK. The results of this analysis are therefore extendable to any radial distribution network that use standard protection, e.g. fuses and relays in low voltage distribution networks. The results were discussed in the light of regulations adopted by the UK, Europe, and the USA. Another result to be highlighted is that the time delay of 0.5 s stipulated by G-83 ensures that sufficient time is available for faults occurring away from the PV to be cleared by the action of the respective fuse, in contrast to 0.16 s stipulated by IEEE 1547:2018. However, a lower cut-off voltage for under-voltage disconnection than stipulated in G-83 would ensure more PV stays connected to the network during a fault that has occurred far from the PV installations.

REFERENCES

- [1] A. P. Reiman, T. E. McDermott, G. F. Reed, and B. Enayati, "Guidelines for high penetration of single-phase PV on power distribution systems," in *Power & Energy Society General Meeting, 2015 IEEE*, 2015, pp. 1-5.
- [2] "Solar Photovoltaics Deployment in the UK, February 2016," Department of Energy and Climate Change 2016.
- [3] J. Machowski, J. W. Bialek, and J. R. Bumby, *Power system dynamics: Stability and Control*, 2nd ed. West Sussex, UK: John Wiley and Sons, 2008.
- [4] KEMA limited, "The contribution to distribution network fault levels from the connection of distributed generation," DTI, London, UK2005.
- [5] L. Freris and D. Infield, *Renewable energy in power systems*. New Jersey, USA: Wiley-Blackwell, 2006.
- [6] S. Conti, "Analysis of distribution network protection issues in presence of dispersed generation," *Electric Power Systems Research*, vol. 79, pp. 49-56, 2009.
- [7] S. S. Kaddah, M. M. El-Saadawi, and D. M. El-Hassanin, "Influence of Distributed Generation on Distribution Networks During Faults," *Electric Power Components and Systems*, vol. 43, pp. 1781-1792, 2015.
- [8] W. Sun, "Maximising Renewable Hosting Capacity in Electricity Networks," Ph. D., University of Edinburgh, Edinburgh, 2015.
- [9] P. T. Manditereza and R. Bansal, "Renewable distributed generation: The hidden challenges – A review from the protection perspective," *Renewable and Sustainable Energy Reviews*, vol. 58, pp. 1457-1465, 2016.
- [10] H. Kobayashi, K. Takigawa, E. Hashimoto, A. Kitamura, and H. Matsuda, "Problems and countermeasures on safety of utility grid with a number of small-scale PV systems," in *IEEE Conference on Photovoltaic Specialists*, Florida, USA, 1990, pp. 850-855 vol.2.

- [11] Intelligent Energy Europe, "State of the art on dispersed PV power generation: Publications review on the impacts of PV Distributed Generation and Electricity networks Annexes," European Commission, Brussels, Germany 2007.
- [12] K. Malmedal, B. Kroposki, and P. K. Sen, "Distributed Energy Resources and Renewable Energy in Distribution Systems: Protection Considerations and Penetration Levels," presented at the IEEE Industry Applications Society Annual Meeting, Edmonton, AB, Canada, 2008.
- [13] J. Keller and B. Kroposki, "Understanding Fault Characteristics of Inverter-Based Distributed Energy Resources," NREL, Colorado, USA 2010.
- [14] C. Le-Thi-Minh, T. Tran-Quoc, S. Bacha, C. Kiény, P. Cabanac, D. Goulielmakis, *et al.*, "Behaviors of photovoltaic systems connected to MV network during faults," presented at the 26th European Photovoltaic Solar Energy Conference and Exhibition, Hamburg, Germany, 2011.
- [15] F. Grumm, M. Plenz, M. F. Meyer, M. Jordan, G. Kaatz, and D. Schulz, "Influence of PV-Systems on Short-Circuit Currents in Low-Voltage Distribution Grids in Structurally Weak Areas," in *2018 IEEE International Conference on Environment and Electrical Engineering and 2018 IEEE Industrial and Commercial Power Systems Europe (EEEIC / I&CPS Europe)*, 2018, pp. 1-6.
- [16] F. Katiraei, J. Holbach, T. Chang, W. Johnson, D. Wills, B. Young, *et al.*, "Investigation of Solar PV Inverters Current Contributions during Faults on Distribution and Transmission Systems Interruption Capacity," presented at the Western Protective Relay Conference, North Carolina, USA, 2012.
- [17] A. P. Reiman, "An analysis of distributed photovoltaics on single-phase laterals of distribution systems," M. Sc., Graduate Faculty of The Swanson School of Engineering, University of Pittsburgh, Pittsburgh, 2015.
- [18] Econnect Ventures Ltd., "Embedded controller for LV networks with distributed generation," DTI, London, UK URN NUMBER: 07/921, 2007.
- [19] S. Ingram, S. Probert, and K. Jackson, "The impact of small scale embedded generation on the operating parameters of distribution networks," P B Power, Department of Trade and Industry, London, UK 2003.
- [20] "Engineering Recommendation G83 - Issue 2," ed: Energy Networks Association, 2012.
- [21] I. Kim, "The effect of load current on a three-phase fault," in *2016 IEEE Power & Energy Society Innovative Smart Grid Technologies Conference (ISGT)*, 2016, pp. 1-4.
- [22] M. Munzinger, F. Crick, E. J. Dayan, N. Pearsall, and C. Martin, "Domestic Photovoltaic Field Trials, Final Technical Report," Building Research Establishment, 2007.
- [23] R. Teodorescu, M. Liserre, and P. Rodriguez, *Grid converters for photovoltaic and wind power systems*. Sussex, UK: John Wiley and Sons Ltd., 2011.
- [24] S. Kouro, J. I. Leon, D. Vinnikov, and L. G. Franquelo, "Grid-Connected Photovoltaic Systems: An Overview of Recent Research and Emerging PV Converter Technology," *IEEE Industrial Electronics Magazine*, vol. 9, pp. 47-61, 2015.
- [25] L. Bowtell and T. Ahfock, "Comparison between unipolar and bipolar single phase gridconnected inverters for PV applications," presented at the Australasian Universities Power Engineering Conference, Perth, WA, Australia, 2007.
- [26] B. Crowhurst, E. F. El-Saadany, L. E. Char, and L. A. Lamont, "Single-Phase Grid-Tie Inverter Control Using DQ Transform for Active and Reactive Load Power Compensation," presented at the IEEE International Conference on Power and Energy, Kuala Lumpur, Malaysia, 2010.
- [27] S. Samerchur, S. Premrudeepeeachacharn, Y. Kumsuwun, and K. Higuchi, "Power control of single-phase voltage source inverter for grid-connected photovoltaic systems," in *Power Systems Conference and Exposition (PSC), 2011 IEEE/PES*, 2011, pp. 1-6.
- [28] J. F. Sultani, "Modelling, design and implementation of d-q control in single-phase grid-connected inverters for photovoltaic systems used in domestic dwellings" Ph. D., Faculty of Technology, De Montfort University, Leicester, 2013.
- [29] Q.-C. Zhong and T. Hornik, *Control of Power Inverters in Renewable Energy and Smart Grid Integration*. New Jersey, USA: Wiley-IEEE press, 2013.
- [30] Energy Networks Association, "Engineering Recommendation G83, Issue 2: Recommendations for the Connection of Type Tested Small-scale Embedded Generators (Up to 16A per Phase) in Parallel with Low-Voltage Distribution Systems," ed. London, UK, 2012.
- [31] F. A. S. Neves, M. Carrasco, F. Mancilla-David, G. M. S. Azevedo, and V. S. Santos, "Unbalanced Grid Fault Ride-Through Control for Single-Stage Photovoltaic Inverters," *IEEE Transactions on power electronics* vol. 31, 2016.
- [32] M. Mirhosseini, J. Pou, and V. G. Agelidis, "Single- and Two-Stage Inverter-Based Grid-Connected Photovoltaic Power Plants With Ride-Through Capability Under Grid Faults," *IEEE Transactions on sustainable energy* vol. 6, 2015.
- [33] R. FARANDA and S. LEVA, "Energy comparison of MPPT techniques for PV Systems," in *WSEAS TRANSACTIONS on POWER SYSTEMS*, Roberto Faranda, Sonia Leva, 2008.
- [34] R. A. Messenger and J. Ventre, *Photovoltaic Systems Engineering*, 3rd ed. London, UK: CRC Press, 2010.
- [35] B. Kroposki and J. Keller, "Understanding Photovoltaic Inverter Fault Current and Low Voltage Ride-Through," presented at the 25th European Photovoltaic Solar Energy Conference and Exhibition, Valencia, Spain, 2010.
- [36] R. K. Aggarwal, N. Ashton, K. A. Coates, P. C. Colbrook, L. Csuros, D. Day, *et al.*, *Power System Protection*, 2 ed. London, UK: The Institution of Electrical Engineers, 1995.
- [37] T. Haggis and A. Land, "Cables, Cable laying and accessories manual," ed. Bristol, UK: Central Networks, 2004.
- [38] Energy Networks Association, "ENA TS 37-2: Substation Cable Distribution Boards," ed. London, UK, 2005.
- [39] Northern Power Grid, "Code of Practice for the economic development of the HV system," ed. Newcastle upon Tyne, UK, 2017.
- [40] "Code of practice 331, Protection of LV Underground and Overhead Distributors and HV Protection of Distribution Transformers," ed: Electricity Northwest Limited, 2014.
- [41] British Standards Institution, "BS EN 60269-2: Low voltage fuses: Supplementary requirement for fuses for use by authorized persons (fuses mainly for industrial applications) - Examples of standardised systems of fuses A to K," ed. London, UK, 2013.
- [42] Northern Power Grid, "Code of Practice for the economic development of the LV system," Newcastle upon Tyne, UK 2017.
- [43] "IEC 61727:2004 - Photovoltaic (PV) systems - Characteristics of the utility interface," ed. Geneva, Switzerland: International Electrotechnical Commission., 2004.
- [44] "IEEE 1547-2003 - IEEE Standard for Interconnecting Distributed Resources with Electric Power Systems," ed. New Jersey, USA: Institute of Electrical and Electronics Engineers, 2003.
- [45] "IEEE 1547-2018 - IEEE Standard for Interconnection and Interoperability of Distributed Energy Resources with Associated Electric Power Systems Interfaces," ed. New Jersey, USA: Institute of Electrical and Electronics Engineers 2018.

'Declarations of interest: none'

Appendix A

Table A provides the details of the typical distribution network representative of the distribution networks in the UK.

Table A: Specifications of the typical distribution network

Component	Specifications
33 kV Source	33 kV source with 500 MVA fault level
33/11.5 kV Transformers	15 MVA 18% impedance on 15 MVA base YY0 windings X/R ratio of 15 Two transformers in parallel -20/20% tap changer with 2.5% tap steps Automatic voltage control scheme with 2.5% bandwidth Voltage set point between 11 and 11.1 kV Off load ratio of 33/11.5 kV
11 kV Feeder circuits	Five feeders modelled with lumped 11 kV – three-phase load of 2 MVA. Power factor same as the sixth detailed feeder.
11 kV detailed feeder circuit	1.5 km of 185 sq. mm. 3 core PICAS plus 1.5 km of 95 sq. mm. 3 core PICAS cable Impedance of 185 sq. mm. is $0.164 + j0.080 \Omega/\text{km}$ Impedance of 95 sq. mm. is $0.32 + j0.087 \Omega/\text{km}$
11/0.433 kV transformer	500 kVA 5% impedance Dy11 windings X/R ratio of 15 Off load ratio of 11/0.433 kV
400 V detailed feeder	Impedance of 240 CNE is $0.1258 + j0.0685 \Omega/\text{km}$ Impedance of 120 CNE is $0.2533 + j0.0685 \Omega/\text{km}$ Impedance of 70 CON is $0.4430 + j0.0705 \Omega/\text{km}$